Journal of Hazardous Materials 190 (2011) 60–68

Contents lists available at ScienceDirect

Journal of Hazardous Materials

journal homepage: www.elsevier.com/locate/jhazmat

Ozonation of imidacloprid in aqueous solutions: Reaction monitoring and identification of degradation products

Marc Bourgin[a,b,c], Frédéric Violleau[c,*], Laurent Debrauwer[d], Joël Albet[a,b]

[a] INRA, UMR 1010, F-31077 Toulouse, France
[b] Université de Toulouse, INPT-ENSIACET, Laboratoire de Chimie Agro-industrielle, 4 Allée Emile Monso, F-31077 Toulouse Cedex 4, France
[c] Université de Toulouse, INPT, Ecole d'Ingénieurs de Purpan, Laboratoire d'Agro-Physiologie, UPSP/DGER 115, 75 Voie du TOEC, BP 57611, F-31076 Toulouse Cedex 3, France
[d] INRA, UMR 1089 Xénobiotiques INRA-ENVT, BP 93173, F-31027 Toulouse Cedex 03, France

ARTICLE INFO

Article history:
Received 30 November 2010
Received in revised form 3 February 2011
Accepted 20 February 2011
Available online 10 March 2011

Keywords:
Ozone
Imidacloprid
Wastewater
Seed loading solution
ESI(+)-MS
Oxidation products

ABSTRACT

This paper presents the degradation of imidacloprid by ozonation. Solutions of 39.0 μg/mL imidacloprid were prepared either by dissolution of standard or by dilution of Gaucho Blé® seed loading solution and then ozonated under different conditions. The concentration of imidacloprid and oxidation products in both solutions was monitored by HPLC-UV as a function of the treatment time for a concentration of 100 g/m^3 of ozone in the inlet gas. No significant difference was observed: in both cases, imidacloprid degradation was a pseudo-first order reaction with similar reaction rates (0.129–0.147 min^{-1}), degradation by-products with the same HPLC retention times were observed and their concentrations as a function of the treatment time followed a very similar trend. The study of ozone concentration in the inlet gas (from 25 to 100 g/m^3) showed that imidacloprid degradation is also a first-order reaction with respect to ozone. The ozonation by-products were then collected and identified by ESI(+)-MS. A degradation pathway of imidacloprid was finally proposed.

1. Introduction

Seeds are constantly threatened by a wide range of pests or pathogen agents at different steps of development: germination, sowing and growth. Consequently, to prevent any disease or attack, seed producers currently treat seeds with water-based formulations containing not only insecticides, fungicides and repellents but also colorants and sticking agents. Imidacloprid (Fig. 1 and Table 1), a neonicotinoid insecticide, is widely applied as a seed treatment (Gaucho®) to control sucking and biting insects (leafhoppers [1,2], aphids [2,3], thrips [4], whiteflies [5], . . .). It was first introduced in 1991 for the treatment of corn [2,6], cereals [3,7,8], sunflower [9], cotton [10], . . .

Seed treatments are usually realized in batch or semi-batch reactors to fulfill a fast and homogeneous treatment. After application, reactors are generally rinsed with water. However, as the amount of pesticides and colorants is very high in seed loading solutions, the contamination and the colorization of the wastewater are dramatic.

Consequently, to solve the problem of the pollution of agricultural wastewaters by pesticides, various treatment processes have been studied: physical treatments (lined evaporative beds and activated carbon adsorption), chemical treatments (photolysis, hydrolysis and chemical oxidation) and biological treatment like activated sludge, biobeds and constructed wetlands [11].

Ozonation, one of the chemical oxidation processes, has been widely investigated for the removal of pesticides [12–15]. Cernigoj et al. [16] studied the degradation of neonicotinoid insecticides but only focused on the ozonation of an imidacloprid analog compound, the thiacloprid. No process of single ozonation of imidacloprid has been investigated yet so far. However, the photo degradation of imidacloprid has been widely studied [17–21] and some degradation products have been identified.

The present study reports the degradation by ozonation of imidacloprid present in a seed loading solution. The aims of this work were as follows: (i) to focus on the decomposition of pesticide; (ii) to highlight the formation of oxidation products by identifying some of them using ESI(+)-MS and (iii) to propose an imidacloprid degradation pathway.

2. Materials and methods

2.1. Chemicals and solvents

Pestanal® grade standard of imidacloprid (>99.0% purity) were purchased from Fluka (Seelze, Germany).

* Corresponding author. Tel.: +33 5 61 15 29 78; fax: +33 5 61 15 30 60.
E-mail address: frederic.violleau@purpan.fr (F. Violleau).

0304-3894/$ – see front matter © 2011 Elsevier B.V. All rights reserved.
doi:10.1016/j.jhazmat.2011.02.065

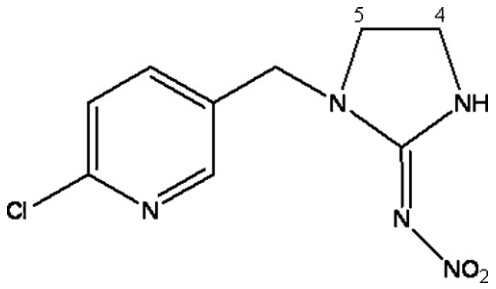

Fig. 1. Chemical structure of imidacloprid.

Acetonitrile (HPLC grade) was purchased from Carlo Erba Reagents-SDS (Val de Reuil, France). Ultrapure water (≥18 MΩ cm resistivity) was obtained from Millipore Simplicity water system (Molsheim, France).

Trifluoroacetic acid (TFA) (*ReagentPlus*®, 99%) was supplied by Sigma–Aldrich (Seelze, Germany).

Gaucho Blé® seed loading solution, containing imidacloprid (in the concentration of 175 g/L) was supplied by Bayer Cropscience (Lyon, France). The concentration of imidacloprid in this solution was 175 g/L but it also contained other pesticides (bitertanol and anthraquinone respectively in the concentration of 37.5 and 125 g/L), colorants, sticking agents, etc.

2.2. Preparation of aqueous solutions of pesticides

Imidacloprid (39.0 μg/mL, ca. 152.9 μM) solutions were prepared after dissolution in ultrapure water–acetonitrile mixture (99:1, v/v). Acetonitrile was used to dissolve pesticides in the solution, as it has a low reactivity with ozone [22].

The seed loading solution was diluted in ultrapure water–acetonitrile mixture (99:1, v/v) to obtain a concentration of imidacloprid of 39.0 μg/mL.

2.3. Ozonation of aqueous solutions of pesticides

A volume of 1.8 L of pesticide stock solution was introduced in a 2-L semi-batch glass reactor and agitated at 400 rpm. A stream of ozone–oxygen mixture gas was bubbled into the solution with a flow rate of 20 L/h and a concentration of ozone of 100 mg/L. Ozone was produced by Ozat CFS-1 ozone generator (Ozonia, Dubendorf, Switzerland) fed by dry pure oxygen (99.5%, Linde Gas). The inlet ozone concentration was continuously determined at 254 nm by UV photometer (BMT 961, BMT Messtechnik, Stahnsdorf, Germany). An overpressure of 200 mbar was maintained in the reactor to increase the dissolution of ozone in the aqueous phase. Dissolved ozone concentration was determined by the indigo colorimetric method [23]. Effluent gases from the reactor were vented to a thermal destruction system (350 °C). Aliquots (10 mL) of ozonated solutions were collected at different treatment times from 0 to 90 min. Residual ozone in aliquots was immediately stripped to quench the reaction by bubbling pure nitrogen for 2 min.

Table 1
Chemical and physical properties of imidacloprid.

Nom	Imidacloprid
Molecular formula	$C_9H_{10}ClN_5O_2$
Molar mass	255.66 g mol^{-1}
Melting point	144 °C
Solubility in water	610 mg L^{-1}

2.4. Analysis and fraction collection of ozonated pesticide solutions

Analysis and fraction collections of ozonated solutions were performed thanks to an HPLC system equipped with a SRD-3400 vacuum membrane degasser, an HPG-3400RS high-pressure binary pump, a WPS-3000TFC autosampler (6-port injection valve, 6-port fractionation valve) and a TCC-3000RS column compartment (Dionex, Sunnyvale, CA). Separations were performed on an analytical column (150 mm × 2.1 mm I.D., 1.7 μm particle size) Kinetex C18 (Phenomenex, Torrance, CA) protected by a Krudkatcher Ultra from Phenomenex (Torrance, CA) equipped with an integrated 0.5 μm 316 stainless steel filter element. Data acquisition and processing were carried out with the Chromeleon version 6.80 software (Dionex, Sunnyvale, CA). All components were detected by a DAD-3000RS diode-array detector (Dionex, Sunnyvale, CA) at the wavelengths of 200, 211, 254 and 270 nm. An aliquot of 20 μL was injected into the HPLC system and eluted at 50 °C, with a flow rate of 0.5 mL/min under the following gradient conditions, where A is 0.1% TFA in ultrapure water and B is acetonitrile: t = 0 min, A–B (95.1:4.9, v/v); t = 18 min, A–B (95.1:4.9, v/v); t = 19 min, A–B (20:80, v/v); t = 29 min, A–B (20:80, v/v); t = 30 min, A–B (95.1:4.9, v/v); t = 48 min, A–B (95.1:4.9, v/v).

Fraction collection was performed after detection of peaks at the wavelength of 254 nm and completion of collection parameters optimized to collect almost only the quantifiable compounds.

2.5. Identification of ozonation by-products

Structural characterization of the purified degradation products was conducted on a LCQ quadrupole ion trap mass spectrometer (Thermo Finnigan, Les Ulis, France) fitted with an electrospray ionization source operated in the positive mode. Collected samples were introduced into the ionization source by infusion at a flow rate of 5 μL/min with a syringe pump. Operating parameters for production and transmission of electrosprayed ions into the ion trap analyzer were optimized for imidacloprid and applied to all the other compounds: needle voltage 5.0 kV; heated capillary temperature 240 °C; capillary voltage 23 V. The sheath gas and auxiliary gas (nitrogen) flow rates were set to respectively 54 and 14 AU (arbitrary units). All other parameters for MS^2 and MS^3 experiments (isolation width, excitation voltage, excitation time) were also adjusted to obtain maximum structural information concerning the compounds of interest.

3. Results and discussion

3.1. Study of the decomposition of imidacloprid in aqueous solution by ozonation

Experiments were conducted by ozonating a solution of standard and a seed loading solution with an initial imidacloprid concentration of 39.0 μg/mL and a concentration of ozone of 100 g/m^3 in the inlet gas. The degradation of imidacloprid in both solutions was monitored by HPLC-DAD and the degradation yield of the compound is summarized in Fig. 2.

It can be seen that the decomposition of imidacloprid started immediately after the ozone was injected in the system. The degradation of imidacloprid was not significantly different in either solution. After 30 min of ozonation, the conversion of imidacloprid was almost complete (superior to 98%) in both solutions.

Then the reaction kinetic regime was investigated and the kinetic order of the reaction was determined. As shown in Fig. 2, a first order kinetic behavior was observed. Indeed, the variation of

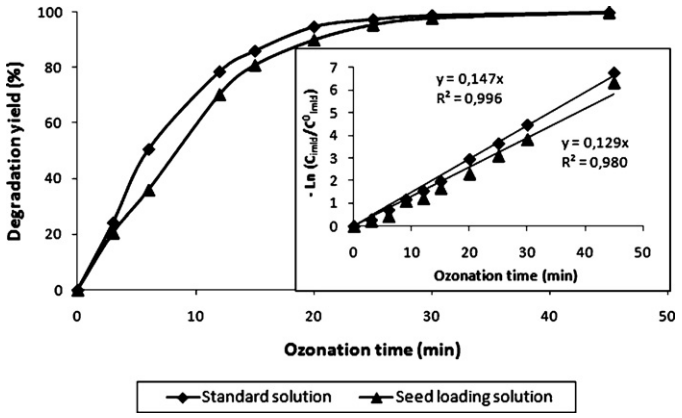

Fig. 2. Evolution of the degradation yield of imidacloprid by ozone in a standard solution (square) and a seed loading solution (triangle) as a function of the treatment time. The inset shows the linear transformation of $\ln(C_{imid}/C^0_{imid})$ as a function of ozonation time for both solutions.

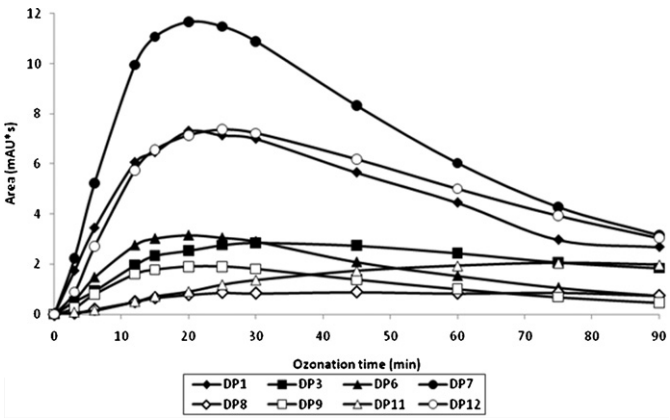

Fig. 4. Evolution of the area of imidacloprid ozonation by-products peaks detected by HPLC-DAD (λ = 254 nm) as a function of treatment time.

$\ln(C_{imid}/C^0_{imid})$, where C_{imid} and C^0_{imid} are respectively the concentration of imidacloprid at any time and at the beginning, with time was linear as the coefficients of determination for the degradation of imidacloprid in both cases were superior to 97.9%. Reaction rate constants were determined graphically and were respectively 0.147 and 0.129 min^{-1} for the standard solution and the seed loading solution, showing a very slight difference of the kinetic between the two types of solutions. Consequently, the decomposition of imidacloprid by ozonation in the diluted seed loading solution did not appear to be limited by the competition of other compounds (other pesticides like bitertanol and anthraquinone or colorants, additives, etc.).

While imidacloprid was decomposed, several ozonation by-products were formed. These products were monitored by their HPLC peak retention times in standard solution and in diluted seed loading solution. The different chromatograms obtained at successive ozonation times indicate that peaks with the same retention times and with similar areas were formed in both solutions (Fig. 3). The evolution of the major peaks (**DP1**, **DP3**, **DP6**, **DP7**, **DP8**, **DP9**, **DP11** and **DP12**) as a function of ozonation time is shown in Fig. 4 for the standard solution. All the peaks appeared as soon as the

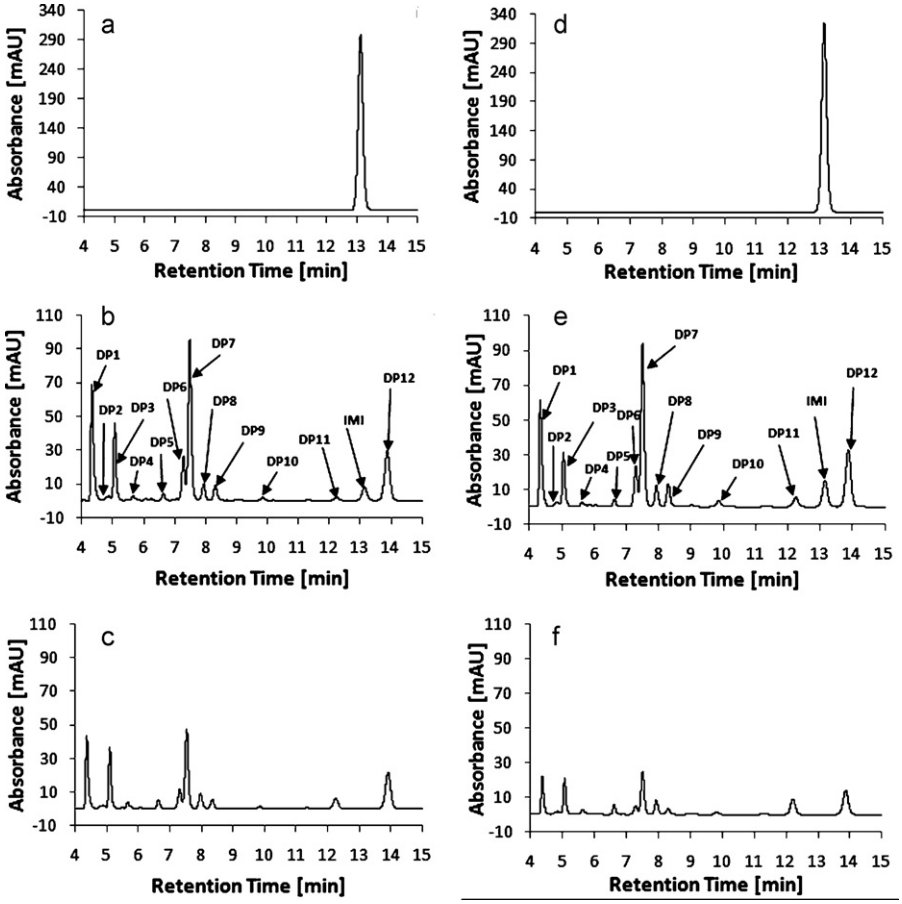

Fig. 3. Chromatograms of ozonated imidacloprid solutions at the wavelength of 254 nm. (a), (b) and (c) represent the chromatograms of a standard solution of imidacloprid respectively after an ozonation time of 0, 25 and 90 min. (d), (e) and (f) represent the chromatograms of a seed loading solution respectively after 0, 25 and 90 min of ozonation.

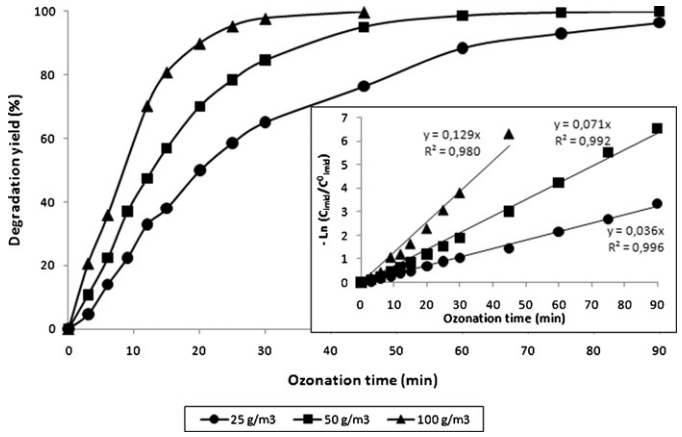

Fig. 5. Evolution of the degradation yield of imidacloprid in a seed loading solution for three concentrations of ozone in the inlet gas: 100 g/m^3 (triangle), 50 g/m^3 (square) and 25 g/m^3 (circle) as a function of the ozonation time. The inset shows the linear transformation of $\ln(C_{imid}/C^0_{imid})$ as a function of treatment time for the 3 concentrations.

ozonation started and three degradation products **DP1, DP7** and **DP12** were rapidly predominant with areas greater than 7 mAU s after 20 min of ozonation. Areas of other by-products did not exceed 4 mAU s. Fig. 4 shows that almost all the major degradation products, except **DP8** and **DP11**, evolved in a similar way with the increasing of their HPLC peaks areas in the first minutes of ozonation to reach a maximum of concentration after 20–25 min. Then, these products were also decomposed by ozone to reach a peak area inferior to 4 mAU s. **DP8** and **DP11** showed a different evolution trend. The areas of both peaks increased all reaction long. The area of **DP5** evolved in the same way as these of **DP8** and **DP11** (data not shown because of the low area of **DP5**).

3.2. Influence of the ozone concentration in the inlet gas on the degradation of imidacloprid

Three different ozone concentrations (25, 50 and 100 g/m^3) were adjusted in the inlet gas for the ozonation of a diluted seed loading solution with an initial imidacloprid concentration of 39.0 μg/mL. The degradation of imidacloprid was monitored for treatment times from 0 to 90 min and shown in Fig. 5.

The decomposition of imidacloprid was complete after 90 min. For the 50 and the 25 g/m^3, the degradation yield was respectively 99.9 and 96.5% after 90 min whereas it was 99.8% for 100 g/m^3 after only 45 min of ozonation (no imidacloprid was detected for superior ozonation times). Consequently, the higher the concentration of ozone in the inlet gas was, the faster the kinetic of decomposition of imidacloprid was.

This information was later confirmed by plotting the variation of $\ln(C_{imid}/C^0_{imid})$ versus time as shown in the inset of Fig. 5. First of all, this figure allowed confirming that the kinetic pseudo-order of the reaction was one as the curves showed a linear trend. Indeed, the coefficients of determination were all superior to 97.9%. Moreover, the kinetic rate constants, calculated as the slope of the curves, were respectively 0.036, 0.071 and 0.129 min^{-1} for an ozone concentration in the inlet gas of 25, 50 and 100 g/m^3. Thus, the kinetic rate constants were approximately doubled following a twofold increase in the concentration of ozone in the inlet gas. Consequently, the reaction appeared to be also of first order for ozone. Thus, the rate law of the ozonation of imidacloprid can be written:

$$r = k_{imid} \cdot C_{O_3(l)} \cdot C_{imid}$$

with k_{imid}, the rate constant of the reaction, $C_{O_3(l)}$ and C_{imid} the concentrations of ozone and imidacloprid in the aqueous solution.

3.3. Identification of ozonation by-products by ESI(+)-MS

The different imidacloprid ozonation by-products were purified by collection. Collected compounds were then analyzed by an ion trap mass spectrometer using positive electrospray ionization mode. For some compounds, authentic standards were available and the identification was achieved by comparing their HPLC retention times, UV spectra and mass spectra at different stages. When standards were not commercially available, the identification of collected compounds was carried out by interpretation of mass spectra.

The full ESI(+)-MS spectra of imidacloprid and its identified degradation products all exhibited a couple of main peaks for the molecular species ($[M+H]^+$ ions), separated by two mass-to-charge ratio (m/z) units, and displaying approximately 100:35 relative abundances, which was indicative of the characteristic isotopic pattern of a chlorinated molecule. Considering the chemical composition of imidacloprid, this information indicated that a chlorine atom was present in all the molecules and so the attack of ozone on imidacloprid did not affect this atom.

All degradation compounds were analyzed using sequential MS and MS/MS experiments into the ion trap device. All the m/z values observed for precursor and fragment ions of the various compounds are summarized in Table 2.

The peak collected at a retention time of 13.2 min and supposed to be imidacloprid was analyzed first and compared with standard of imidacloprid. For both compounds, MS spectral data were identical. A key m/z was the precursor ion at m/z 256 (Table 2). Collisional excitation of the m/z 256 ion gave rise to different fragment ions at m/z 212, m/z 210, m/z 209 and m/z 175 (corresponding to a loss of 44, 46, 47 and 81 mass units with respect to the precursor ion). Fragment ions at m/z 210 and 209 were respectively formed by the loss of NO_2 radical and HNO_2 from precursor ion. The formation of the ion at m/z 212 has already been reported in the literature [24,25]. Although no mechanism of fragmentation has been proposed, Blasco et al. [24] attributed its formation to the loss of N_2O. According to the structure of imidacloprid, a rearrangement of the ion to a urea derivative was suggested. A fragmentation scheme of the nitroguanidine group of imidacloprid is proposed in Fig. 6. Afterwards, the loss of 44, 46 and 47 m/z units on the precursor ions of imidacloprid and of degradation products was assumed to originate in the fragmentation of nitroguanidine group and was thus considered as an indicator of the presence of the nitroguanidine group in the precursor ion. A difference of 35 m/z units between fragment ions at m/z 210 and m/z 175 pointed out a loss of chlorine radical ^{35}Cl.

The ESI(+)-MS spectrum of **DP1** displays $[M+H]^+$ ion at m/z 231. The mass-selection and subsequent fragmentation of the m/z 231 ion yielded a main product ion at m/z 169. According to the nitrogen rule, the change in the mass parity compared to imidacloprid indicated a change in the number of nitrogen atoms in the molecule, possibly by an oxidation of the nitroguanidine group. This assumption was confirmed by the absence of fragment ions at m/z ratios corresponding to $[\mathbf{DP1}+H-44]^+$, $[\mathbf{DP1}+H-46]^+$ and $[\mathbf{DP1}+H-47]^+$. However, the MS data were not sufficient to characterize this degradation product.

The $[M+H]^+$ ion of **DP2** was detected at m/z 142 (Table 2). Data obtained from this product were compared to those of 6-chloronicotinaldehyde. Both products presented similar HPLC retention time, UV spectrum, MS and MS^2 spectra showing a fragment ion at m/z 124. **DP2** was thus identified as 6-chloronicotinaldehyde.

Table 2
Precursor ions and fragment ions with their relative abundance (*A*, %) at different MS stages for the degradation products of imidacloprid. n.d.: not determined.

Compound	MS		MS^2			MS^3	
	m/z $[M+H]^+$		m/z (*A*, %)	Neutral loss		m/z (*A*, %)	Neutral loss
DP1	231	→	169 (100)	n.d.	→	151 (100)	n.d.
DP2	142	→	124 (100)	$[-H_2O]$			
DP3	230	→	186 (100)	$[-N_2O]$	→	169 (100)	$[-NH_3]$
			184 (11)	$[-NO_2]$			
			148 (8)	$[-NO_2,-HCl]$			
DP4	288	→	244 (100)	$[-N_2O]$	→	226 (54)	$[-H_2O]$
			242 (11)	$[-NO_2]$		208 (22)	$[-2H_2O]$
			207 (11)	$[-NO_2,-Cl]$		186 (14)	$[-C_2H_2O_2]$
			206 (27)	$[-NO_2,-HCl]$		169 (100)	$[-C_2H_2O_2,-NH_3]$
						144 (38)	$[-C_3H_4O_2N_2]$
DP5	158	→	140 (100)	$[-H_2O]$			
DP6	208	→	166 (14)	n.d.			
			127 (100)	n.d.			
			126 (22)	n.d.			
DP7	272	→	228 (100)	$[-N_2O]$	→	210 (77)	$[-H_2O]$
			226 (49)	$[-NO_2]$		169 (24)	$[-C_2H_2O,-NH_3]$
			191 (22)	$[-NO_2,-Cl]$		144 (100)	$[-C_3H_4ON_2]$
			190 (50)	$[-NO_2,-HCl]$		126 (12)	$[-C_3H_4ON_2,-H_2O]$
DP8	240	→	169 (100)	n.d.			
			126 (13)	n.d.			
DP9	270	→	226 (100)	$[-N_2O]$	→	208 (14)	$[-H_2O]$
			224 (8)	$[-NO_2]$		126 (100)	$[-C_3H_3N_2O_2]$
			189 (7)	$[-NO_2,-Cl]$		113 (33)	$[-Cl(C_5H_4N)]$
DP10	270	→	226 (15)	$[-N_2O]$		140 (100)	$[-C_3H_6N_2O]$
			224 (4)	$[-NO_2]$			
			223 (100)	$[-HNO_2]$	→		
DP11	286	→	268 (46)	$[-H_2O]$		224 (18)	$[-H_2O]$
			242 (100)	$[-N_2O]$	→	199 (13)	[–HNCO]
			240 (12)	$[-NO_2]$		169 (100)	$[-C_2H_3O_2N]$
			239 (13)	$[-HNO_2]$		126 (27)	$[-C_3H_4O_3N_2]$
IMI	256	→	212 (34)	$[-N_2O]$		175 (100)	[–Cl]
			210 (100)	$[-NO_2]$	→		
			209 (23)	$[-HNO_2]$			
			175 (21)	$[-NO_2,-Cl]$			
DP12	270	→	226 (100)	$[-N_2O]$	→	208 (10)	$[-H_2O]$
						190 (9)	[–HCl]
						169 (10)	$[-C_2H_3NO]$
						126 (100)	$[-C_3H_3N_2O_2]$
						114 (57)	$[-Cl(C_5H_4N),+H]$
						113 (44)	$[-Cl(C_5H_4N)]$
DP13	143	→	126 (100)	$[-NH_3]$			

The analysis of **DP3** by ESI(+)-MS enabled to detect an $[M+H]^+$ ion at m/z 230, supposed to be the product formed by the opening of imidazolidine ring. Tandem mass spectrometric experiments carried out on the m/z 230 ion gave rise to fragment ions at m/z 186, m/z 184 and m/z 148, corresponding to the loss of N_2O, NO_2 and NO_2 + HCl respectively. Mass-selection and collision-induced dissociation of the m/z 186 ion in a further MS^3 experiment yielded a main product ion at m/z 169 (loss of NH_3). Structures

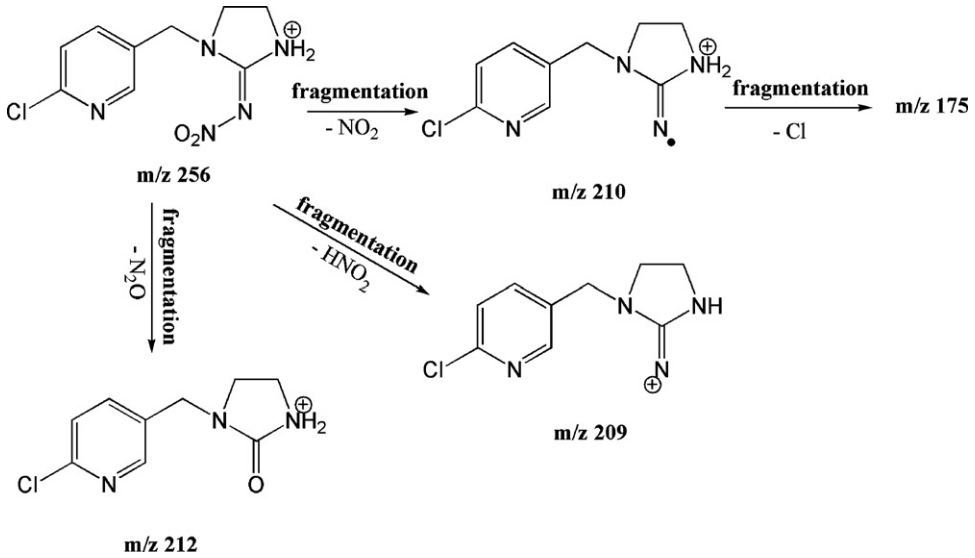

Fig. 6. Fragmentation pathways proposed for imidacloprid analyzed by ESI(+)-MS/MS.

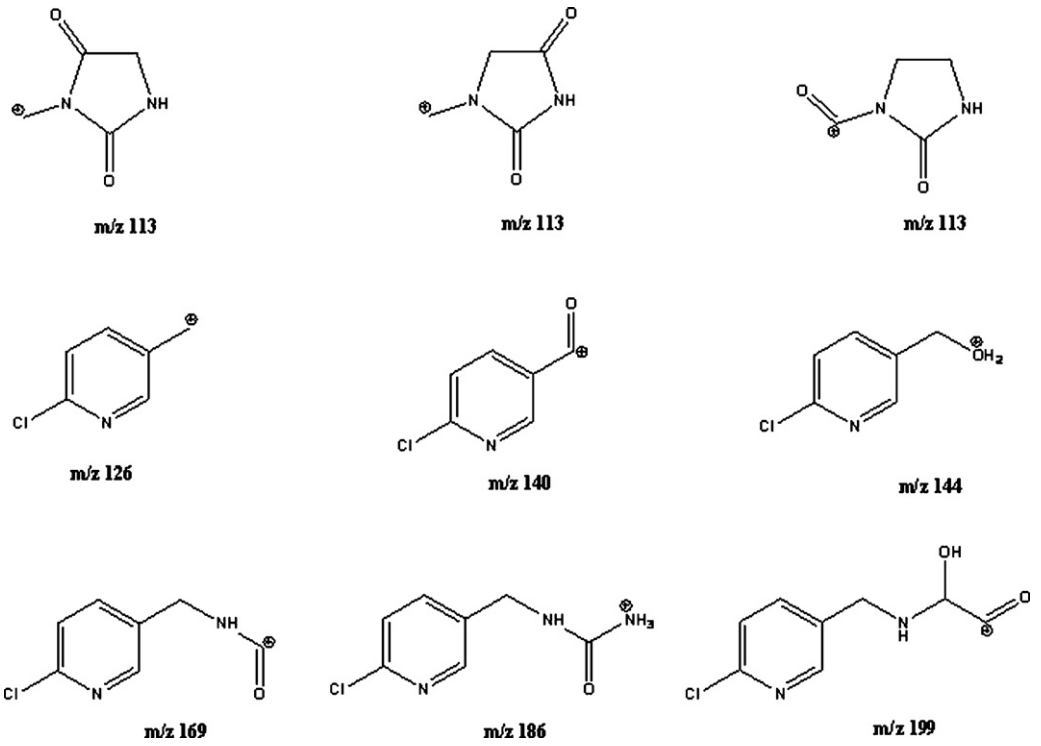

Fig. 7. Proposed structures for characteristic fragment ions found in the MS^3 spectra of imidacloprid degradation products and used for their identification.

are proposed in Fig. 7 for both fragment ions at *m*/*z* 186 and *m*/*z* 169.

The MS spectrum of **DP4** displayed a $[M+H]^+$ ion at *m*/*z* 288, which could be attributed to a dihydroxylated form of imidacloprid. Due to the chemical structure of imidacloprid, three different structures were considered (**DP4a**, **DP4b** and **DP4c**, see Fig. 8). Tandem mass spectrometry on the precursor ion showed a fragmentation leading to *m*/*z* 244 ($[\mathbf{DP4}+H-N_2O]^+$) and *m*/*z* 242 ($[\mathbf{DP4}+H-NO_2]^+$) ions, corresponding to the fragmentation of the nitroguanidine moiety, and to *m*/*z* 207 and *m*/*z* 206 ions, associated to the consecutive losses of NO_2 and chlorine. The mass-selection and fragmentation of the main fragment ion at *m*/*z* 244 led to the *m*/*z* 186 and *m*/*z* 169 ions (see structures proposed in Fig. 7), already discussed for **DP3**. The fragmentation of the *m*/*z* 244 ion $[\mathbf{DP4}+H-N_2O]^+$ also led to fragment ions at *m*/*z* 226 ion ($[\mathbf{DP4}+H-N_2O-H_2O]^+$) and *m*/*z* 208 ion ($[\mathbf{DP4}+H-N_2O-2H_2O]^+$). For this latter ion, the possible formation of a $[\mathbf{DP4}+H-N_2O-HCl]^+$ ion was ruled out because similar MS^3 experiments carried out on the ^{37}Cl isotopic ion at *m*/*z* 290 yielded a *m*/*z* 210 fragment ion, indicating that the chlorine atom was still present. A fragment ion at *m*/*z* 144, for which a structure is proposed in Fig. 7, was also observed in the MS^3 mass spectrum of **DP4**, indicating that imidacloprid was hydroxylated on the alkyl group outside the imidazolidine ring. However, data were not sufficient to locate the second hydroxyl

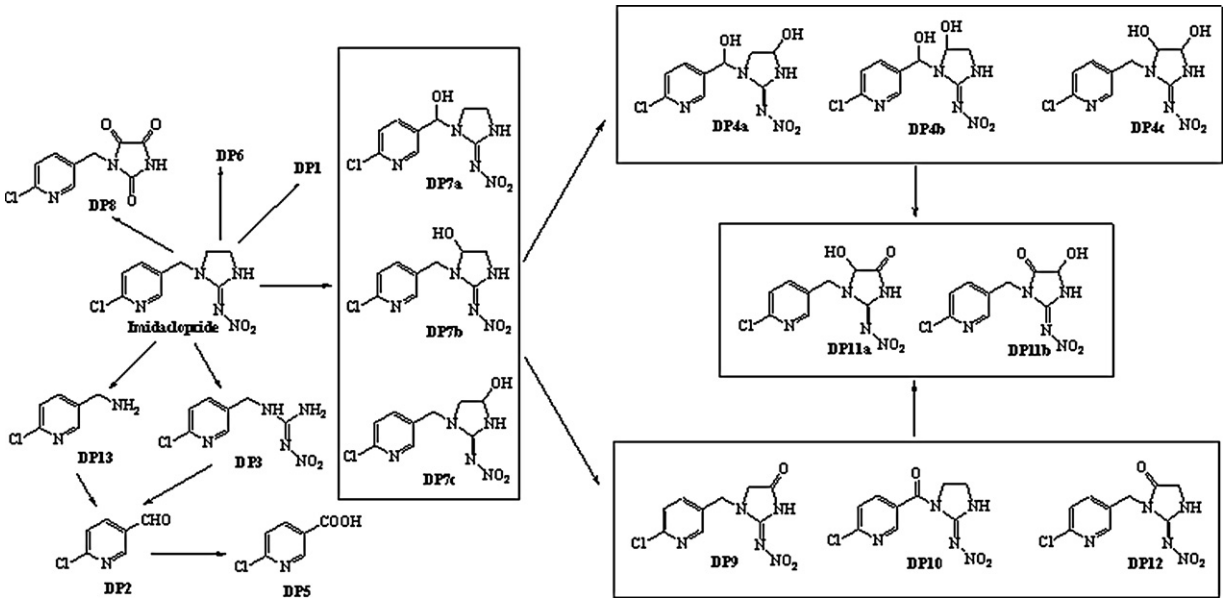

Fig. 8. Proposed degradation pathways of imidacloprid by ozonation.

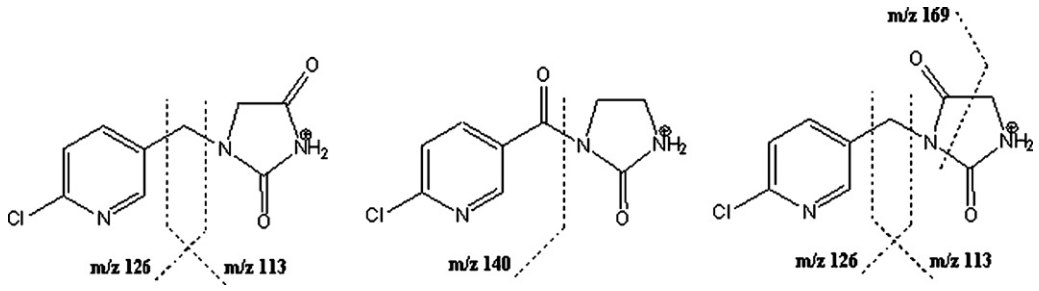

Fig. 9. Proposed fragmentation pathways of the *m/z* 226 daughter ions formed from the ESI-produced *m/z* 270 parent ions.

group as well as to reject the possible presence of the **DP4c** product in the collected peak.

When analyzed by ESI(+)-MS, **DP5** yielded a $[M+H]^+$ ion displaying a mass-to-charge ratio of 158, equivalent to that of 6-chloronicotinic acid. The collected peak and standard 6-chloronicotinic acid led to similar HPLC retention times, UV and mass spectral data. The *m/z* 158 precursor ion gave a daughter ion at *m/z* 140, corresponding to the loss of H_2O. Consequently, **DP5** was assigned to 6-chloronicotinic acid.

The MS spectrum of **DP6** showed a major ion at *m/z* 209, corresponding to $[\mathbf{DP6}+H]^+$ (Table 2). As for all other compounds, the ^{37}Cl isotopic peak was observed (*m/z* 211), giving the characteristic isotopic pattern of a mono-chlorinated compound. The *m/z* 209 ion was selected and fragmented into the ion trap device. Fragment ions at *m/z* 173 and *m/z* 126 were strongly predominant in the resulting MS^2 spectrum. The change in the parity of precursor ion's mass-to-charge ratio indicated a change in the number of nitrogen atoms in the molecule, possibly *via* an oxidation of the nitroguanidine group. Besides, no loss of 44, 46 or 47 mass units from the precursor ion was observed, suggesting that the nitroguanidine moiety was probably modified. The *m/z* 173 fragment ion likely resulted from the elimination of HCl from the *m/z* 209 parent ion, while the *m/z* 126 fragment ion most probably corresponded to the structure proposed in Fig. 7. Based on these data, it could be deduced that the chloro-pyridylmethyl moiety of imidacloprid remained unchanged in **DP6**, while the N-nitro-imidazolidine-2-ylidenamine substructure likely underwent the loss of the nitro group to yield an imidazoline-2-ylidenamine type structure. However, these available data were not sufficient to complete the unambiguous identification of **DP6**.

The analysis of **DP7** by ESI(+)-MS enabled to prove an $[M+H]^+$ ion at *m/z* 272 (^{35}Cl isotopic contribution). This could correspond to compounds formed by monohydroxylation of imidacloprid, which were expected to be present in the collected fractions. Nevertheless, three compounds could have been formed (**DP7a**, **DP7b** and **DP7c**, Fig. 8). MS/MS experiments performed on the *m/z* 272 ion gave rise to fragment ions at *m/z* 228 and *m/z* 226 (loss of N_2O and NO_2 respectively) and at *m/z* 191 and *m/z* 190, which could be attributed to the consecutive loss of chlorine and hydrogen chloride respectively from the *m/z* 226 ion. Mass-selection and subsequent fragmentation of the *m/z* 228 ion mainly yielded the *m/z* 210 ion, by loss of the neutral H_2O, and the *m/z* 144 ion already observed in the MS^3 spectrum of dihydroxylated imidacloprid **DP4** (Fig. 7). The occurrence of this fragment ion indicated that imidacloprid was hydroxylated on the alkyl group outside the imidazolidine ring (**DP7a**, Fig. 8). However, data in the mass spectra did not allow concluding a complete regioselectivity of hydroxylation of imidacloprid, and the occurrence of the other possible hydroxylated forms (**DP7b**, **DP7c**, Fig. 8) in the collected fraction corresponding to **DP7** could not be ruled out. Consequently, the three structures proposed earlier were proposed for the collected compound **DP7**.

The MS spectrum of **DP8** showed an $[M+H]^+$ ion at *m/z* 240. After isolation and fragmentation by tandem mass spectrometry, main fragment ions were observed at *m/z* 169 and *m/z* 126 in the resulting MS^2 spectrum (see proposed structures in Fig. 7). This spectrum did not display any fragment ion corresponding to the loss of 44, 46 and 47 mass units from the precursor ion, indicating that the nitroguanidine moiety was probably oxidized. The occurrence of the *m/z* 126 ion indicated that the chloro-pyridylmethyl moiety was not modified whereas the *m/z* 169 ion suggested that at least one carbonyl group was present on the imidazolidine moiety of the studied compound. The additional mass-selection and excitation of the *m/z* 169 ion did not give significant fragmentation. According to the collected spectral data, a compound displaying an imidazolidine-2,4,5-one moiety, as indicated in Fig. 8, could be proposed as a possible structure for **DP8**.

The **DP9**, **DP10** and **DP12** collected peaks were also analyzed by ESI(+)-MS. All three of them yielded an $[M+H]^+$ ion at *m/z* 270 (Table 2), that could correspond to carbonylated forms of imidacloprid. Mass-selection and fragmentation of the *m/z* 270 ion gave rise to fragment ions at *m/z* 226, *m/z* 224 and/or *m/z* 223, associated to the fragmentation of the nitroguanidine moiety (loss of N_2O, NO_2 and HNO_2 respectively). The information obtained from the MS^2 spectrum was not sufficient to identify the position of carbonyl group on each molecule. Consequently, ESI(+)-MS^3 analyses were conducted on the major fragment ions from the three oxidation products. The mass-selection and collision-induced dissociation of the *m/z* 226 ion gave two main fragment ions at *m/z* 126 and at *m/z* 113 (see Table 2). The presence of the fragment at *m/z* 113 could be explained by the loss of the pyridine moiety, yielding the structure proposed in Fig. 7. However, this *m/z* 113 fragment ion was not indicative of the position of the carbonyl group in the molecule. Nevertheless, this information was provided by the presence or the absence of specific fragment ions at *m/z* 126, *m/z* 140 and *m/z* 169, presented in Fig. 7. Indeed, the occurrence of the *m/z* 140 fragment ion indicates that the carbonylation took place on the alkyl group outside the imidazolidine ring. On the contrary, the presence of the *m/z* 126 ion together with the absence of the *m/z* 140 ion in the MS^3 spectrum points out that the carbonyl group is present on the imidazolidine ring (Fig. 9), as observed for **DP9** and **DP12**. On the other hand, the MS^3 spectrum of **DP10** displayed a major fragment ion at *m/z* 140, indicating that the carbonyl group is located on the alkyl group out of the imidazolidine group. Finally, the MS^3 spectrum of **DP12** showed three major peaks at *m/z* 169, *m/z* 126 and *m/z* 113. The peak at *m/z* 126 pointed out that the carbonyl group was located on the imidazolidine ring. Moreover, the presence of the *m/z* 169 fragment ion – absent in the MS^3 spectra of **DP9** and **DP10** – was rather indicative of a carbonylation on the position 5 on the imidazolidine ring, as described in Fig. 9. Alternatively, the absence of the *m/z* 169 fragment ion for **DP9** would allow deducing this compound was carbonylated on the position 4 of the imidazolidine ring. Based on this information, structures were proposed for **DP9**, **DP10** and **DP12** as reported in Fig. 8. Unlike the monohydroxylated compounds **DP7**, the carbonylated derivatives were well separated by HPLC with the developed analytical conditions. By considering the chromatograms of the ozonated imi-

dacloprid solutions and by normalizing the response coefficients of the carbonylated compounds, it can be assumed that the products **DP9** and **DP12**, *i.e.* the compound carbonylated on the imidazolidine ring, were predominantly formed, compared to the product carbonylated outside the ring **DP10**.

The analysis of **DP11** by ESI(+)-MS showed an $[M+H]^+$ ion at *m/z* 286, that could correspond to the occurrence of both an hydroxylated and a carbonylated position on imidacloprid. According to the structure of imidacloprid, six different products were first considered. The collision-induced dissociation of the *m/z* 286 ion gave rise to fragment ions at *m/z* 268, *m/z* 242, *m/z* 240 and *m/z* 239. The fragment ion at *m/z* 268 was most probably formed by the loss of H_2O, confirming the presence of an hydroxyl group in the structure of **DP11**, while the 3 other fragment ions should correspond to the fragmentation of the nitroguanidine moiety, by the loss of N_2O (ion at *m/z* 242), NO_2 (ion at *m/z* 240) and HNO_2 (ion at *m/z* 239), indicating that the nitroguanidine moiety remained unchanged. The MS^3 fragmentation of the major fragment ion at *m/z* 242 yielded fragment ions at *m/z* 224, *m/z* 199, *m/z* 169 and *m/z* 126. The first fragment ion was probably formed by the loss of H_2O. Both the presence of the *m/z* 126 ion and the absence of the *m/z* 144 and 140 ions indicated that the functionalization of imidacloprid (hydroxylation and/or carbonylation) did not occur on the methyl group of the chloro-pyridylmethyl moiety but rather on both alkyl groups on the imidazolidine ring. Furthermore, the presence of the *m/z* 169 fragment ion suggested that the carbonyl group was likely located on the position 5 of the imidazolidine ring, implying the hydroxylation located on the position 4 (**DP11b**). However, the occurrence of a fragment ion at *m/z* 199, presented in Fig. 7, may have originated in the fragmentation of a compound hydroxylated on the position 5 and carbonylated on the position 4 (**DP11a**). Consequently, it was concluded that the collected peak for **DP11** likely corresponds to a mixture of two co eluted isomers, namely **DP11a** and **DP11b**.

The parameters used for the collection enabled retrieving some non quantifiable peaks, especially the compound **DP13**, characterized by a very low HPLC retention time (1.4 min) and by an $[M+H]^+$ ion at *m/z* 143. Fragmentation of this ion by tandem mass spectrometry gave a fragment ion at *m/z* 126 (see Fig. 7). The spectral data and HPLC retention time were found to fit these of standard 5-(amino methyl)-2-chloropyridine. Thus **DP13** was identified as 5-(amino methyl)-2-chloropyridine (8).

3.4. Mechanism of degradation

Imidacloprid has, on its imidazolidine ring, two amine groups that could have been oxidized by hydroxylation on the α carbon of amine groups [26] to yield the products **DP7**. It has already been reported, in the literature, that the formation of monohydroxylated imidacloprid is mainly metabolic and microbial transformation [27–30]. The monohydroxylated imidacloprid could react with ozone in four different ways: (i) by a second hydroxylation on another α carbon to yield **DP4**; (ii) by oxidation of alcohol to carbonyl group to form **DP9**, **DP10** and **DP12**; (iii) by a combined oxidation of the alcohol function and hydroxylation to yield **DP11**; (iv) by N-dealkylation of amines to form an opened-ring compound **DP3**.

The presence of the three carbonylated compounds **DP9**, **DP10** and **DP12** indicates that the first step of hydroxylation was probably not selective and occurred on the three alkyl groups of imidacloprid to form the three isomers of monohydroxylated imidacloprid.

N-dealkylated products **DP3** and **DP13** are precursor compounds in the formation of the aldehyde **DP12**, according to the mechanisms described by Bailey [31] and Elmghari-Tabib [32]. The aldehyde was probably further oxidized to 6-chloronicotinic acid **DP5**. This compound has already been reported to be formed during oxidative treatment of imidacloprid but it has not been generally very reactive. Consequently, it was not surprising to notice that the concentration of **DP5** increased during all the ozonation time.

The different proposals of degradation pathways of imidacloprid are summarized in Fig. 8.

4. Conclusions

Imidacloprid was decomposed in an aqueous standard solution and in a seed loading solution. The degradation was similar in both cases: the kinetic of the reactions was of the same order and the by-products formed during the ozonation, were the same, and in the same proportions. Thus the components present in the seed loading solution matrix did not have significant effects on the degradation of imidacloprid by ozonation. Thirteen degradation products were collected and analyzed by ESI(+)-MS, among which 11, could be characterized by interpretation of the data obtained by multi-dimensional mass spectrometric experiments. As for the remaining 2 compounds, only a mass-to-charge ratio could be obtained. Finally, a degradation pathway of imidacloprid by ozone was proposed.

Acknowledgements

This work has been financially supported by the company Epi de Gascogne (Francescas, France) and the French Ministry (ANRT).

References

[1] B.A. Nault, A.G. Taylor, M. Urwiler, T. Rabaey, W.D. Hutchison, Neonicotinoid seed treatments for managing potato leafhopper infestations in snap bean, Crop Prot. 23 (2004) 147–154.
[2] X. Pons, R. Albajes, Control of maize pests with imidacloprid seed dressing treatment in Catalonia (NE Iberian Peninsula) under traditional crop conditions, Crop Prot. 21 (2002) 943–950.
[3] S.M. Gray, G.C. Bergstrom, R. Vaughan, D.M. Smith, D.W. Kalb, Insecticidal control of cereal aphids and its impact on the epidemiology of the barley yellow dwarf luteoviruses, Crop Prot. 15 (1996) 687–697.
[4] A. Ester, R. de Vogel, E. Bouma, Controlling Thrips tabaci (Lind.) in leek by film-coating seeds with insecticides, Crop Prot. 16 (1997) 673–677.
[5] F.J. Byrne, R.D. Oetting, J.A. Bethke, C. Green, J. Chamberlin, Understanding the dynamics of neonicotinoid activity in the management of Bemisia tabaci whiteflies on poinsettias, Crop Prot. 29 (2010) 260–266.
[6] T.P. Kuhar, L.J. Stivers-Young, M.P. Hoffmann, A.G. Taylor, Control of corn flea beetle and Stewart's wilt in sweet corn with imidacloprid and thiamethoxam seed treatments, Crop Prot. 21 (2002) 25–31.
[7] N.E. Ahmed, H.O. Kanan, S. Inanaga, Y.Q. Ma, Y. Sugimoto, Impact of pesticide seed treatments on aphid control and yield of wheat in the Sudan, Crop Prot. 20 (2001) 929–934.
[8] L.C. Simms, A. Ester, M.J. Wilson, Control of slug damage to oilseed rape and wheat with imidacloprid seed dressings in laboratory and field experiments, Crop Prot. 25 (2006) 549–555.
[9] R. Schmuck, R. Schöning, A. Stork, O. Schramel, Risk posed to honeybees (Apis mellifera L., Hymenoptera) by an imidacloprid seed dressing of sunflowers, Pest Manag. Sci. 57 (2001) 225–238.
[10] S.E. El-Hamady, R. Kubiak, A.S. Derbalah, Fate of imidacloprid in soil and plant after application to cotton seeds, Chemosphere 71 (2008) 2173–2179.
[11] K. Ikehata, M.G. El-Din, Aqueous pesticide degradation by hydrogen peroxide/ultraviolet irradiation and Fenton-type advanced oxidation processes: a review, J. Environ. Eng. Sci. 5 (2006) 81–135.
[12] K. Ikehata, M.G. El-Din, Aqueous pesticide degradation by ozonation and ozone-based advanced oxidation processes: a review (Part I), Ozone: Sci. Eng. 27 (2005) 83–114.
[13] K. Ikehata, M.G. El-Din, Aqueous pesticide degradation by ozonation and ozone-based advanced oxidation processes: a review (Part II), Ozone: Sci. Eng. 27 (2005) 173–202.
[14] G. Reynolds, N. Graham, R. Perry, R.G. Rice, Aqueous ozonation of pesticides: a review, Ozone: Sci. Eng. 11 (1989) 339–382.
[15] J. Lawrence, F.P. Cappelli, Ozone in drinking water treatment: a review, Sci. Total Environ. 7 (1977) 99–108.
[16] U. Cernigoj, U.L. Stangar, P. Trebse, Degradation of neonicotinoid insecticides by different advanced oxidation processes and studying the effect of ozone on TiO_2 photocatalysis, Appl. Catal. B 75 (2007) 229–238.
[17] S. Malato, J. Caceres, A. Aguera, M. Mezcua, D. Hernando, J. Vial, A.R. Fernandez-Alba, Degradation of imidacloprid in water by photo-Fenton and TiO_2 photocatalysis at a solar pilot plant: a comparative study, Environ. Sci. Technol. 35 (2001) 4359–4366.

[18] S. Malato, J. Blanco, J. Cáceres, A.R. Fernández-Alba, A. Agüera, A. Rodríguez, Photocatalytic treatment of water-soluble pesticides by photo-Fenton and TiO_2 using solar energy, Catal. Today 76 (2002) 209–220.
[19] H. Fallmann, T. Krutzler, R. Bauer, S. Malato, J. Blanco, Applicability of the photo-Fenton method for treating water containing pesticides, Catal. Today 54 (1999) 309–319.
[20] H. Fallmann, T. Krutzler, R. Bauer, S. Malato, J. Blanco, Detoxification of pesticide containing effluents by solar driven Fenton process, Z. Phys. Chem. 213 (1999) 67–74.
[21] A. Berneker, Untersuchungen zum Verhalten von insektizidhaltigen Wässern bei Prozessen der chemischen Naßoxidation, Universität Bremen, 1999.
[22] C.C.D. Yao, W.R. Haag, Rate constants for direct reactions of ozone with several drinking water contaminants, Water Res. 25 (1991) 761–773.
[23] H. Bader, J. Hoigné, Determination of ozone in water by the indigo method, Water Res. 15 (1981) 449–456.
[24] C. Blasco, M. Fernandez, Y. Pico, G. Font, J. Mañes, Simultaneous determination of imidacloprid, carbendazim, methiocarb and hexythiazox in peaches and nectarines by liquid chromatography–mass spectrometry, Anal. Chim. Acta 461 (2002) 109–116.
[25] S. Liu, Z. Zheng, F. Wei, Y. Ren, W. Gui, H. Wu, G. Zhu, Simultaneous determination of seven neonicotinoid pesticide residues in food by ultraperformance liquid chromatography tandem mass spectrometry, J. Agric. Food Chem. 58 (2010) 3271–3278.
[26] H.B. Henbest, M.J.W. Stratford, Amine oxidation. Part VIII. The reaction of tri-n-butylamine with ozone, J. Chem. Soc. (1964) 711–714.
[27] F.M. Laurent, E. Rathahao, Distribution of [14C]imidacloprid in sunflowers (Helianthus annuus L.) following seed treatment, J. Agric. Food Chem. 51 (2003) 8005–8010.
[28] R. Nauen, U. Ebbinghaus-Kintscher, R. Schmuck, Toxicity and nicotinic acetylcholine receptor interaction of imidacloprid and its metabolites in Apis mellifera (Hymenoptera: Apidae), Pest Manag. Sci. 57 (2001) 577–586.
[29] D.A. Schulz-Jander, J.E. Casida, Imidacloprid insecticide metabolism: human cytochrome P450 isozymes differ in selectivity for imidazolidine oxidation versus nitroimine reduction, Toxicol. Lett. 132 (2002) 65–70.
[30] S. Suchail, G. De Sousa, R. Rahmani, L.P. Belzunces, In vivo distribution and metabolisation of 14C-imidacloprid in different compartments of Apis mellifera L., Pest Manag. Sci. 60 (2004) 1056–1062.
[31] P.S. Bailey, D.A. Michard, A.-I.Y. Kashhab, Ozonation of amines. II. Competition between amine oxide formation and side-chain oxidation, J. Org. Chem. 33 (1968) 2675–2680.
[32] M. Elmghari-Tabib, Ozonation reaction patterns of alcohols and aliphatic amines, Ozone: Sci. Eng. 4 (1982) 195–205.